J. Phys.: Condens. Matter **23** (2011) 234101 (11pp) doi:10.1088/0953-8984/23/23/234101

# Electrostatic models of electron-driven proton transfer across a lipid membrane

**Anatoly Yu Smirnov**[1,2], **Lev G Mourokh**[3] **and Franco Nori**[1,2]

[1] Advanced Science Institute, RIKEN, Wako-shi, Saitama, 351-0198, Japan
[2] Physics Department, The University of Michigan, Ann Arbor, MI 48109-1040, USA
[3] Department of Physics, Queens College, The City University of New York, Flushing, NY 11367, USA

Received 8 August 2010
Published 25 May 2011
Online at stacks.iop.org/JPhysCM/23/234101

**Abstract**

We present two models for electron-driven uphill proton transport across lipid membranes, with the electron energy converted to the proton gradient via the electrostatic interaction. In the first model, associated with the *cytochrome c oxidase* complex in the inner mitochondria membranes, the electrostatic coupling to the site occupied by an electron lowers the energy level of the proton-binding site, making proton transfer possible. In the second model, roughly describing the redox loop in a nitrate respiration of *E. coli* bacteria, an electron displaces a proton from the negative side of the membrane to a shuttle, which subsequently diffuses across the membrane and unloads the proton to its positive side. We show that both models can be described by the same approach, which can be significantly simplified if the system is separated into several clusters, with strong Coulomb interaction inside each cluster and weak transfer couplings between them. We derive and solve the equations of motion for the electron and proton creation/annihilation operators, taking into account the appropriate Coulomb terms, tunnel couplings, and the interaction with the environment. For the second model, these equations of motion are solved jointly with a Langevin-type equation for the shuttle position. We obtain expressions for the electron and proton currents and determine their dependence on the electron and proton voltage build-ups, on-site charging energies, reorganization energies, temperature, and other system parameters. We show that the quantum yield in our models can be up to 100% and the power-conversion efficiency can reach 35%.

(Some figures in this article are in colour only in the electronic version)

## 1. Introduction

Every living organism obtains the energy needed for its survival from the outside world. This energy can be in the form of sunlight or food; but in both cases it is unstable and cannot be utilized directly, so several energy-conversion steps are necessary. One of the most widely used intermediate forms for energy storage is the electrochemical proton gradient across lipid membranes, such as the inner mitochondrial membranes or plasma membranes in bacteria. To achieve and maintain this proton gradient, Nature employs several different types of electron- or light-driven systems, where the energy of high-energetic electrons or absorbed photons is used for the energetically uphill proton transfer from the negative (N) to the positive (P) sides of the membrane.

Here we discuss two mechanisms of energy conversion from the highly unstable electronic form of energy to the proton gradient, namely, proton pumps and redox loops [1, 2]. Both mechanisms rely on the electrostatic interaction between electrons and protons, although the specific details of the proton pumps and the redox loops look very different. For example, in a proton pump, such as *cytochrome c oxidase*, electrons move mainly along the membrane, whereas protons move across the membrane, which results in an accumulation of the positive charge on the P-side and in the generation of a proton-motive force (PMF) [3–6]. In the redox-loop mechanism of PMF generation, taking place in the nitrate respiratory chain of the *E. coli* bacterium, the *neutral shuttle*, carrying *both* protons and electrons, crosses the membrane. Here, charge accumulation occurs when electrons cross the

 

membrane, just before embarking on the shuttle, and right after unloading from the shuttle [7–12]. It should be noted that the proton pump operating in the *cytochrome c oxidase* has no essential mechanically moving parts, whereas the redox-loop mechanism is impossible without the molecular shuttle diffusing between the N and the P sides of the lipid membrane.

In general, the treatment of the electron and proton transfer events is extremely difficult because the total number of occupation states increases exponentially with the number of electron- and proton-binding sites, when all of them are electrostatically coupled. In the present work, however, we show that both above-mentioned mechanisms of the transmembrane proton translocation can be described with a similar mathematical model, taking into account the Coulomb interaction between *one* electron- and *one* proton-binding sites only, and neglecting electrostatic couplings to other sites. It is necessary to have at least three redox sites and three proton-binding sites in order to obtain a proton pumping effect and suppress a reverse flow of protons from the P-side to the 'N'-side of the membrane. In the absence of strong Coulomb interaction between all sites, there is no need to introduce a complete set of electron and proton occupation states (as was done in our previous works, [6, 11–13]), which grows exponentially with the number of sites. Instead, we now divide the whole system into clusters of strongly coupled sites. These clusters are described by their own set of occupation states, and the total number of states in the system is equal to the sum (not the product!) of the states in the clusters. The clusters are weakly coupled by electron tunneling terms and by proton transfer amplitudes, so that transitions between the clusters can be considered within perturbation theory. While in this work we present quite simple models, similar approaches can be applied to much more complicated biological systems, such as Photosystem II and the whole respiratory chain in the inner mitochondrial membrane [2].

The quantum yield for the two models analyzed in this paper can be about 1. Why such a high quantum yield? This can be explained from the fact that, in order to be transferred through the system, an electron needs to lose its energy. This cannot be done via the environment because the reorganization energy is not large enough. Consequently, electron transport occurs with the assistance of protons gaining this energy and being transferred to the P-side of the membrane. Thus, the transfer of a single electron is accompanied by the transfer of a single proton and the corresponding currents are equal, which results in an almost perfect quantum yield.

## 2. Model

We consider a physical model describing an electron-coupled translocation of protons from the N- to the P-side of a membrane. The model consists of an interaction site, $Q = \{Q_e, Q_p\}$, containing a single electron level with energy $\varepsilon_Q$ and a single proton energy level characterized by the energy $E_Q$. We also introduce two electron sites, L and R, coupled to the electron site $Q_e$, and two proton sites, A and B, coupled to the proton site $Q_p$ (figure 1). The electron site L is coupled to the electron source (S), and the site R is connected to the electron drain (D). The proton site A is coupled to the proton reservoir N (the negative side of the membrane), and the site B is coupled to the positive side of the membrane (proton reservoir P).

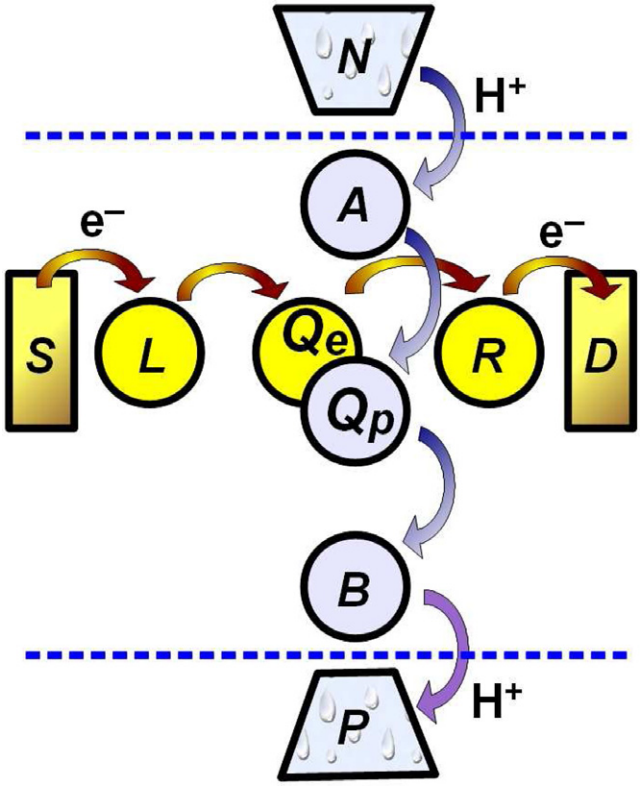


**Figure 1.** Schematic diagram of the static proton pump. The electron-transport chain starts at the source (S) lead. Thereafter, high energy electrons, $e^-$, tunnel *energetically downhill* (through the yellow path) to the sites L, $Q_e$, R and, finally, to the drain (D). Low energy protons, $H^+$, move *energetically uphill* (in blue) from the N-side of the membrane to the sites A, $Q_p$, B and, eventually, reach the P-side of the membrane.

### 2.1. Hamiltonian

The Coulomb interaction between an electron and a proton, both located on the central site Q, is described by the energy $u_0$, so that the Hamiltonian of the site Q has the form

$$H_Q = \varepsilon_Q n_Q + E_Q N_Q - u_0 n_Q N_Q, \tag{1}$$

where $n_Q = a_Q^\dagger a_Q$ is the electron population of the site Q, and $N_Q = b_Q^\dagger b_Q$ is the proton population of this site. Electrons are described by the Fermi-operators $a_\sigma$, and protons are characterized by the Fermi-operators $b_\alpha$ with $\sigma = L, Q_e, R$ and $\alpha = A, Q_p, C$, and with the corresponding populations $n_\sigma = a_\sigma^\dagger a_\sigma$, $N_\alpha = b_\alpha^\dagger b_\alpha$.

The contribution of the electron sites L, R and the proton sites A, B to the total Hamiltonian of the system is described by the term

$$H_0 = \varepsilon_L n_L + \varepsilon_R n_R + E_A N_A + E_B N_B, \tag{2}$$

where $\varepsilon_L$, $\varepsilon_R$ are the energy levels of the electron sites L and R, and $E_A$, $E_B$ are the energies of the proton-binding sites A and B.

The strongly interacting electron and proton sites $Q_e$ and $Q_p$ form a single (interaction) cluster, whereas the sites L, R and A, B separately form another four (peripheral) clusters. The cluster Q can be characterized by the vacuum (empty) state and by three additional occupation states, or, equivalently, by the average electron and proton populations, $\langle n_Q\rangle$ and $\langle N_Q\rangle$, complemented by the correlation function, $K = \langle n_Q N_Q\rangle$. The other electron and proton clusters are described by the corresponding average occupations, $\langle n_L\rangle, \langle n_R\rangle$ and $\langle N_A\rangle, \langle N_B\rangle$. For six electron and proton-binding sites we should have $2^6 = 64$ occupation states. However, with the cluster approach, the system can be completely described by only seven functions: $\langle n_Q\rangle, \langle N_Q\rangle, K$ (for the interaction cluster), and $\langle n_L\rangle, \langle n_R\rangle, \langle N_A\rangle, \langle N_B\rangle$ (for the peripheral clusters). Previously, we applied a similar approach to analyze quantum transport problems in nanomechanical systems [14].

*2.1.1. Electron and proton transitions.* The electron tunneling Hamiltonian between the site Q and the sites L and R is given by

$$H_e = -\Delta_L\, a_L^\dagger\, a_Q - \Delta_R\, a_R^\dagger\, a_Q + \text{h.c.}, \tag{3}$$

whereas the A–Q and B–Q proton transitions are described by the term

$$H_p = -\Delta_A\, b_A^\dagger\, b_Q - \Delta_B\, b_B^\dagger\, b_Q + \text{h.c.}. \tag{4}$$

Here $\Delta_L, \Delta_R$ are the electron tunneling coefficients, and $\Delta_A, \Delta_B$ are the proton transfer amplitudes. In the case of a movable interaction site, e.g., when the electron and proton sites Q are located on the shuttle (quinone/quinol), the amplitudes $\Delta_L, \Delta_R$ and $\Delta_A, \Delta_B$ depend on the position $x$ of the shuttle.

The S-lead serves as a source of electrons, and the D-lead works as an electron drain. The coupling to these leads is characterized by the Hamiltonian

$$H_{LR} = -\sum_k t_{kS}\, c_{kS}^\dagger\, a_L - \sum_k t_{kD}\, c_{kD}^\dagger\, a_R + \text{h.c.}. \tag{5}$$

The proton transitions between the N-side of the membrane and the site A and between the P-side of the membrane and the site B are described by the Hamiltonian

$$H_{AB} = -\sum_q T_{qN}\, d_{qN}^\dagger\, b_A - \sum_q T_{qP}\, d_{qP}^\dagger\, b_C + \text{h.c.}. \tag{6}$$

Here $c_{kS}, c_{kD}$ are Fermi operators of the electron reservoirs S and D, and $d_{qN}, d_{qP}$ are the Fermi operators of protons in the reservoirs N and P. The electron reservoirs S and D have the Hamiltonian

$$H_{SD} = \sum_k (\varepsilon_{kS}\, c_{kS}^\dagger\, c_{kS} + \varepsilon_{kD}\, c_{kD}^\dagger\, c_{kD}), \tag{7}$$

and are characterized by the Fermi distributions $f_S(\varepsilon_{kS})$, $f_D(\varepsilon_{kD})$ with the corresponding electrochemical potentials $\mu_S$ and $\mu_D$. For the proton reservoirs N and P we have the Hamiltonian

$$H_{NP} = \sum_q (E_{qN}\, d_{qN}^\dagger\, d_{qN} + E_{qP}\, d_{qP}^\dagger\, d_{qP}), \tag{8}$$

with the Fermi distributions $F_N(E_{qN})$ and $F_P(E_{qP})$ and the proton electrochemical potentials $\mu_N$ and $\mu_P$.

*2.1.2. Environment.* The interaction of the electron–proton system with the protein environment, which is described as a sum of independent oscillators [15], is characterized by the Hamiltonian

$$\begin{aligned} H_{env} = \sum_j \frac{p_j^2}{2m_j} + \sum_j \frac{m_j\omega_j^2}{2}\Bigg(x_j - \sum_\sigma x_{j\sigma} n_\sigma \\ - x_{jS}\sum_k c_{kS}^\dagger c_{kS} - x_{jD}\sum_k c_{kD}^\dagger c_{kD} \\ - \sum_\alpha X_{j\alpha} N_\alpha - X_{jN}\sum_q d_{qN}^\dagger d_{qN} - X_{jP}\sum_q d_{qP}^\dagger d_{qP}\Bigg)^2, \end{aligned} \tag{9}$$

where $n_\sigma = a_\sigma^\dagger a_\sigma$ is the population of the electron site $\sigma$ ($\sigma = L, Q, R$), $N_\alpha = b_\alpha^\dagger b_\alpha$ is the population of the proton site $\alpha$ ($\alpha = A, Q, B$). The constants $x_{j\sigma}, x_{jS}, x_{jD}$ determine the electron coupling to the environment, and the parameters $X_{j\alpha}, X_{jN}, X_{jP}$ describe the proton–environment interaction.

With the unitary transformation,

$$\begin{aligned} \mathcal{U} = \exp\Bigg[-\mathrm{i}\sum_j p_j\Bigg(\sum_\sigma x_{j\sigma} n_\sigma \\ + x_{jS}\sum_k c_{kS}^\dagger c_{kS} + x_{jD}\sum_k c_{kD}^\dagger c_{kD} \\ + \sum_\alpha X_{j\alpha} N_\alpha + X_{jN}\sum_q d_{qN}^\dagger d_{qN} + X_{jP}\sum_q d_{qP}^\dagger d_{qP}\Bigg)\Bigg], \end{aligned} \tag{10}$$

the Hamiltonian of the environment can be rewritten as

$$H_{env} = \sum_j \left(\frac{p_j^2}{2m_j} + \frac{m_j\omega_j^2 x_j^2}{2}\right), \tag{11}$$

whereas the Hamiltonians $H_e$ and $H_p$ acquire the stochastic phase factors:

$$H_e = -\Delta_L\, \mathrm{e}^{\mathrm{i}\xi_L}\, a_L^\dagger\, a_Q - \Delta_R\, \mathrm{e}^{\mathrm{i}\xi_R}\, a_R^\dagger\, a_Q + \text{h.c.}, \tag{12}$$

and

$$H_p = -\Delta_A\, \mathrm{e}^{\mathrm{i}\xi_A}\, b_A^\dagger\, b_Q - \Delta_B\, \mathrm{e}^{\mathrm{i}\xi_B}\, b_B^\dagger\, b_Q + \text{h.c.}, \tag{13}$$

with the phases

$$\xi_L = \sum_j p_j (x_{jL} - x_{jQ}),$$

$$\xi_R = \sum_j p_j (x_{jR} - x_{jQ}),$$

and

$$\xi_A = \sum_j p_j (X_{jA} - X_{jQ}),$$

$$\xi_B = \sum_j p_j (X_{jB} - X_{jQ}).$$

For simplicity, we assume that there are no phase shifts for the electron transitions between the electron source S and the site L, and the electron drain D and the site R, so that $x_{jS} = x_{jL}$, and $x_{jD} = x_{jR}$, with the same assumption for the N–A and P–B proton transitions, $X_{jN} = X_{jA}$ and $X_{jP} = X_{jB}$.

### 2.2. Rate equations

The time evolution of the electron operators $n_\sigma$ is determined by the Heisenberg equations:

$$\begin{aligned}\dot{n}_{\rm L} &= {\rm i}\Delta_{\rm L}\,{\rm e}^{{\rm i}\xi_{\rm L}}\,a_{\rm L}^\dagger\,a_{\rm Q} - {\rm i}\sum_k t_{k{\rm S}}\,c_{k{\rm S}}^\dagger\,a_{\rm L} + {\rm h.c.},\\ \dot{n}_{\rm R} &= {\rm i}\Delta_{\rm R}\,{\rm e}^{{\rm i}\xi_{\rm R}}\,a_{\rm R}^\dagger\,a_{\rm Q} - {\rm i}\sum_k t_{k{\rm D}}\,c_{k{\rm D}}^\dagger\,a_{\rm R} + {\rm h.c.},\end{aligned} \tag{14}$$

and

$$\dot{n}_{\rm Q} = -{\rm i}\Delta_{\rm L}\,{\rm e}^{{\rm i}\xi_{\rm L}}\,a_{\rm L}^\dagger\,a_{\rm Q} - {\rm i}\Delta_{\rm R}\,{\rm e}^{{\rm i}\xi_{\rm R}}\,a_{\rm R}^\dagger\,a_{\rm Q} + {\rm h.c.}. \tag{15}$$

For the proton populations $N_\alpha$, we derive a similar set of Heisenberg equations,

$$\begin{aligned}\dot{N}_{\rm A} &= {\rm i}\Delta_{\rm A}\,{\rm e}^{{\rm i}\xi_{\rm A}}\,b_{\rm A}^\dagger\,b_{\rm Q} - {\rm i}\sum_q T_{q{\rm N}}\,d_{q{\rm N}}^\dagger\,b_{\rm A} + {\rm h.c.},\\ \dot{N}_{\rm B} &= {\rm i}\Delta_{\rm B}\,{\rm e}^{{\rm i}\xi_{\rm B}}\,b_{\rm B}^\dagger\,b_{\rm Q} - {\rm i}\sum_q T_{q{\rm P}}\,d_{q{\rm P}}^\dagger\,b_{\rm B} + {\rm h.c.}.\end{aligned} \tag{16}$$

This set should be complemented by the equation for the proton population of the interaction site,

$$\dot{N}_{\rm Q} = -{\rm i}\Delta_{\rm A}\,{\rm e}^{{\rm i}\xi_{\rm A}}\,b_{\rm A}^\dagger\,b_{\rm Q} - {\rm i}\Delta_{\rm B}\,{\rm e}^{{\rm i}\xi_{\rm B}}\,b_{\rm B}^\dagger\,b_{\rm Q} + {\rm h.c.}, \tag{17}$$

as well as by the equations for the operators of electron and proton reservoirs,

$${\rm i}\,\dot{c}_{k{\rm S}} = \varepsilon_{k{\rm S}}\,c_{k{\rm S}} - t_{k{\rm S}}\,a_{\rm L}, \qquad {\rm i}\,\dot{c}_{k{\rm D}} = \varepsilon_{k{\rm D}}\,c_{k{\rm D}} - t_{k{\rm D}}\,a_{\rm R}, \tag{18}$$

$${\rm i}\,\dot{d}_{q{\rm N}} = E_{q{\rm N}}\,d_{q{\rm N}} - T_{q{\rm N}}\,b_{\rm A}, \qquad {\rm i}\,\dot{d}_{q{\rm P}} = E_{q{\rm P}}\,d_{q{\rm P}} - T_{q{\rm P}}\,b_{\rm B}. \tag{19}$$

*2.2.1. Contribution of reservoirs to the rate equations.* It follows from equation (18) that the electron operator $c_{k{\rm S}}$ can be represented as

$$c_{k{\rm S}} = c_{k{\rm S}}^{(0)} - t_{k{\rm S}}\int {\rm d}t_1\,\langle -{\rm i}[c_{k{\rm S}}^{(0)}(t), c_{k{\rm S}}^{(0)\dagger}(t_1)]_+\rangle\,a_{\rm L}(t_1)\,\theta(t-t_1), \tag{20}$$

where $c_{k{\rm S}}^{(0)}(t)$ is the free variable of the S-lead, and $\theta(t-t_1)$ is the Heaviside step function. Similar expressions exist for the electron operator $c_{k{\rm D}}(t)$ and for the operators $d_{q{\rm N}}, d_{q{\rm P}}$ of the proton reservoirs. For the weak coupling between the reservoir S and the electron site L we obtain

$$\begin{aligned}\langle a_{\rm L}^\dagger(t)c_{k{\rm S}}^{(0)}(t)\rangle &= -{\rm i}t_{k{\rm S}}\int {\rm d}t_1\,\langle c_{k{\rm S}}^{(0)\dagger}(t_1)c_{k{\rm S}}^{(0)}(t)\rangle\\ &\quad\times\langle [a_{\rm L}(t_1), a_{\rm L}^\dagger(t)]_+\rangle\,\theta(t-t_1).\end{aligned} \tag{21}$$

Thus, the contribution of the S-lead to the evolution of the average electron population $\langle n_{\rm L}\rangle$ (see equation (14)) is determined by the expression

$$\begin{aligned}{\rm i}\sum_k t_{k{\rm S}}^*\langle a_{\rm L}^\dagger(t)c_{k{\rm S}}(t)\rangle &= -\sum_k |t_{k{\rm S}}|^2\\ &\quad\times\int {\rm d}t_1\{\langle c_{k{\rm S}}^{(0)}(t)c_{k{\rm S}}^{(0)\dagger}(t_1)\rangle\,\langle a_{\rm L}^\dagger(t)a_{\rm L}(t_1)\rangle\\ &\quad-\langle c_{k{\rm S}}^{(0)\dagger}(t_1)c_{k{\rm S}}^{(0)}(t)\rangle\,\langle a_{\rm L}(t_1)a_{\rm L}^\dagger(t)\rangle\}.\end{aligned} \tag{22}$$

The correlator $\langle c_{k{\rm S}}^{(0)\dagger}(t_1)c_{k{\rm S}}^{(0)}(t)\rangle$ is proportional to the Fermi distribution function, $f_{\rm S}(\varepsilon_{k{\rm S}})$ of electrons in the reservoir S,

$$\langle c_{k{\rm S}}^{(0)\dagger}(t_1)c_{k{\rm S}}^{(0)}(t)\rangle = f_{\rm S}(\varepsilon_{k{\rm S}})\,{\rm e}^{-{\rm i}\varepsilon_{k{\rm S}}(t-t_1)}, \tag{23}$$

where the Fermi function,

$$f_{\rm S}(\varepsilon) = \left[\exp\left(\frac{\varepsilon-\mu_{\rm S}}{T}\right)+1\right]^{-1},$$

is characterized by the electrochemical potential $\mu_{\rm S}$ and temperature $T$. We assume that the site L is weakly coupled to the reservoir S and to the site Q, thus, we can use free-evolving operators,

$$a_{\rm L}(t) = {\rm e}^{-{\rm i}\varepsilon_{\rm L}(t-t_1)}\,a_{\rm L}(t_1),$$

to calculate the corresponding correlation functions in equation (22), e.g.,

$$\langle a_{\rm L}^\dagger(t)\,a_{\rm L}(t_1)\rangle = \langle n_{\rm L}(t)\rangle\,{\rm e}^{{\rm i}\varepsilon_{\rm L}(t-t_1)}.$$

Introducing the energy-independent rate constant,

$$\gamma_{\rm S} = 2\pi\sum_k |t_{k{\rm S}}|^2\,\delta(\varepsilon_{\rm L}-\varepsilon_{k{\rm S}}), \tag{24}$$

we calculate the contribution of the S-lead to the time evolution of the population $\langle n_{\rm L}\rangle$,

$${\rm i}\sum_k t_{k{\rm S}}^*\,\langle a_{\rm L}^\dagger(t)c_{k{\rm S}}(t)\rangle + {\rm H.c.} = \gamma_{\rm S}\,[f_{\rm S}(\varepsilon_{\rm L}) - \langle n_{\rm L}\rangle]. \tag{25}$$

The same analysis can be applied for a calculation of contributions of the electron lead D and the proton leads N and P to the corresponding populations $\langle n_{\rm R}\rangle$ and $\langle N_{\rm A}\rangle$, $\langle N_{\rm P}\rangle$. The proton transfer rates between the sites A and C and the N and P sides of the membrane, respectively, are determined by the coefficients $\Gamma_{\rm N}$ and $\Gamma_{\rm P}$ where, e.g.,

$$\Gamma_{\rm N} = 2\pi\sum_q |T_{q{\rm N}}|^2\,\delta(E_{\rm A}-E_{q{\rm N}}). \tag{26}$$

*2.2.2. Contribution of site-to-site tunneling to the rate equations.* To calculate the contribution of the L–Q tunneling to the evolution of the populations $\langle n_{\rm L}\rangle$ and $\langle n_{\rm Q}\rangle$, we start with the amplitude $a_{\rm Q}$, which obeys the equation

$${\rm i}\dot{a}_{\rm Q} = \varepsilon_{\rm Q}\,a_{\rm Q} - u_0\,N_{\rm Q}\,a_{\rm Q} - \Delta_{\rm L}^*\,{\rm e}^{-{\rm i}\xi_{\rm L}}\,a_{\rm L} - \Delta_{\rm R}^*\,{\rm e}^{-{\rm i}\xi_{\rm R}}\,a_{\rm R}. \tag{27}$$

In the case of weak L–Q and R–Q tunnel couplings, the formal solution of equation (27) can be written in the form

$$\begin{aligned}a_{\rm Q}(t) &= a_{\rm Q}^{(0)}(t) - \int {\rm d}t_1\,\langle -{\rm i}[a_{\rm Q}^{(0)}(t), a_{\rm Q}^{(0)\dagger}(t_1)]_+\rangle\\ &\quad\times\{\Delta_{\rm L}^*\,{\rm e}^{-{\rm i}\xi_{\rm L}(t_1)}\,a_{\rm L}(t_1) + \Delta_{\rm R}^*\,{\rm e}^{-{\rm i}\xi_{\rm R}(t_1)}\,a_{\rm R}(t_1)\},\end{aligned} \tag{28}$$

where $a_{\rm Q}^{(0)}(t)$ is the free operator of the site Q, obeying the equation (27) with the tunneling terms neglected ($\Delta_{\rm L} = 0$, $\Delta_{\rm R} = 0$).

Taking into account the formula

$$\begin{aligned}{\rm i}\Delta_{\rm L}\,\langle {\rm e}^{{\rm i}\xi_{\rm L}}\,a_{\rm L}^\dagger\,a_{\rm Q}^{(0)}\rangle &= |\Delta_{\rm L}|^2\int {\rm d}t_1\,\langle a_{\rm Q}^{(0)\dagger}(t_1)a_{\rm Q}^{(0)}(t)\rangle\\ &\quad\times\langle [{\rm e}^{{\rm i}\xi_{\rm L}}(t)\,a_{\rm L}^\dagger(t), {\rm e}^{-{\rm i}\xi_{\rm L}(t_1)}\,a_{\rm L}(t_1)]_+\rangle\,\theta(t-t_1),\end{aligned} \tag{29}$$

which is similar to equation (21), we obtain

$$\begin{aligned} \mathrm{i}\Delta_{\mathrm{L}}\,\langle \mathrm{e}^{\mathrm{i}\xi_{\mathrm{L}}}\, a_{\mathrm{L}}^{\dagger}\, a_{\mathrm{Q}}\rangle = |\Delta_{\mathrm{L}}|^2 \int \mathrm{d}t_1\, \{\langle \mathrm{e}^{-\mathrm{i}\xi_{\mathrm{L}}(t_1)}\, \mathrm{e}^{\mathrm{i}\xi_{\mathrm{L}}(t)}\rangle \\ \times \langle a_{\mathrm{Q}}^{\dagger}(t_1)\, a_{\mathrm{Q}}(t)\rangle\, \langle a_{\mathrm{L}}(t_1)\, a_{\mathrm{L}}^{\dagger}(t)\rangle \\ - \langle \mathrm{e}^{\mathrm{i}\xi_{\mathrm{L}}(t)}\, \mathrm{e}^{-\mathrm{i}\xi_{\mathrm{L}}(t_1)}\rangle\, \langle a_{\mathrm{Q}}(t)\, a_{\mathrm{Q}}^{\dagger}(t_1)\rangle\, \langle a_{\mathrm{L}}^{\dagger}(t)\, a_{\mathrm{L}}(t_1)\rangle\}. \end{aligned} \tag{30}$$

Dropping the label $^{(0)}$, we assume that the time evolution of the operators $a_{\mathrm{Q}}$ in equation (30) is calculated with the free-evolution formula,

$$\begin{aligned} a_{\mathrm{Q}}(t) = \mathrm{e}^{-\mathrm{i}\varepsilon_{\mathrm{Q}}(t-t_1)}\, a_{\mathrm{Q}}(t_1) \\ - \mathrm{e}^{-\mathrm{i}\varepsilon_{\mathrm{Q}}(t-t_1)}\, [1 - \mathrm{e}^{\mathrm{i}u_0(t-t_1)}]\, N_{\mathrm{Q}}(t_1)\, a_{\mathrm{Q}}(t_1). \end{aligned} \tag{31}$$

For the free-evolving proton operator of the interaction site we obtain a similar expression

$$\begin{aligned} b_{\mathrm{Q}}(t) = \mathrm{e}^{-\mathrm{i}E_{\mathrm{Q}}(t-t_1)}\, b_{\mathrm{Q}}(t_1) \\ - \mathrm{e}^{-\mathrm{i}E_{\mathrm{Q}}(t-t_1)}\, [1 - \mathrm{e}^{\mathrm{i}u_0(t-t_1)}]\, n_{\mathrm{Q}}(t_1)\, b_{\mathrm{Q}}(t_1). \end{aligned} \tag{32}$$

The influence of the environment on the electron tunneling between the sites L and Q, and between the sites R and Q, is determined by the correlators $\langle \mathrm{e}^{-\mathrm{i}\xi_{\mathrm{L}}(t_1)}\, \mathrm{e}^{\mathrm{i}\xi_{\mathrm{L}}(t)}\rangle$ and $\langle \mathrm{e}^{\mathrm{i}\xi_{\mathrm{L}}(t)}\, \mathrm{e}^{-\mathrm{i}\xi_{\mathrm{L}}(t_1)}\rangle$, where

$$\langle \mathrm{e}^{\mathrm{i}\xi_{\mathrm{L}}(t)}\, \mathrm{e}^{-\mathrm{i}\xi_{\mathrm{L}}(t_1)}\rangle = \exp\{-\mathrm{i}\lambda_{\mathrm{L}}(t-t_1)\}\, \exp\{-\lambda_{\mathrm{L}} T (t-t_1)^2\}. \tag{33}$$

The reorganization energy, $\lambda_{\mathrm{L}}$, is defined as [15]

$$\lambda_{\mathrm{L}} = \sum_j \frac{m_j \omega_j^2}{2} (x_{j\mathrm{L}} - x_{j\mathrm{Q}})^2. \tag{34}$$

The electron reorganization energy $\lambda_{\mathrm{R}}$, and the proton reorganization energies $\Lambda_{\mathrm{A}}$ and $\Lambda_{\mathrm{B}}$, are defined in a similar way. In particular,

$$\Lambda_{\mathrm{A}} = \sum_j \frac{m_j \omega_j^2}{2} (X_{j\mathrm{A}} - X_{j\mathrm{Q}})^2. \tag{35}$$

*2.2.3. Equations for populations of electron- and proton-binding sites.* Consequently, we derive the system of rate equations for the average populations of the electron sites,

$$\begin{aligned} \dot{n}_{\mathrm{L}} + \gamma_{\mathrm{S}} n_{\mathrm{L}} = \gamma_{\mathrm{S}} f_{\mathrm{S}}(\varepsilon_{\mathrm{L}}) + \Phi_{\mathrm{L}}, \\ \dot{n}_{\mathrm{R}} + \gamma_{\mathrm{D}} n_{\mathrm{R}} = \gamma_{\mathrm{D}} f_{\mathrm{D}}(\varepsilon_{\mathrm{R}}) + \Phi_{\mathrm{R}}, \\ \dot{n}_{\mathrm{Q}} = -\Phi_{\mathrm{L}} - \Phi_{\mathrm{R}}, \end{aligned} \tag{36}$$

and for the average populations of the proton-binding sites,

$$\begin{aligned} \dot{N}_{\mathrm{A}} + \Gamma_{\mathrm{N}} N_{\mathrm{A}} = \Gamma_{\mathrm{N}} F_{\mathrm{N}}(E_{\mathrm{A}}) + \Phi_{\mathrm{A}}, \\ \dot{N}_{\mathrm{B}} + \Gamma_{\mathrm{P}} N_{\mathrm{B}} = \Gamma_{\mathrm{P}} F_{\mathrm{P}}(E_{\mathrm{B}}) + \Phi_{\mathrm{B}}, \\ \dot{N}_{\mathrm{Q}} = -\Phi_{\mathrm{A}} - \Phi_{\mathrm{B}}. \end{aligned} \tag{37}$$

Here $\Phi_\sigma$ ($\sigma = \mathrm{L}, \mathrm{R}$) and $\Phi_\alpha$ ($\alpha = \mathrm{A}, \mathrm{B}$) are the functions of the average electron and proton populations, respectively. In addition, due to a strong electron–proton Coulomb interaction on the site Q, the kinetic terms $\Phi_\sigma$ and $\Phi_\alpha$ depend on the correlation function,

$$\langle K\rangle = \langle n_{\mathrm{Q}}(t) N_{\mathrm{Q}}(t)\rangle, \tag{38}$$

of the electron and proton populations on the site Q,

$$\begin{aligned} \Phi_\sigma = \kappa_\sigma(\varepsilon_\sigma - \varepsilon_{\mathrm{Q}} + \lambda_\sigma)\langle n_{\mathrm{Q}}\rangle\langle 1 - n_\sigma\rangle \\ - \kappa_\sigma(\varepsilon_\sigma - \varepsilon_{\mathrm{Q}} - \lambda_\sigma)\langle 1 - n_{\mathrm{Q}}\rangle\langle n_\sigma\rangle \\ + \{\kappa_\sigma(\varepsilon_\sigma - \varepsilon_{\mathrm{Q}} + u_0 + \lambda_\sigma) - \kappa_\sigma(\varepsilon_\sigma - \varepsilon_{\mathrm{Q}} + \lambda_\sigma)\} \\ \times \langle 1 - n_\sigma\rangle\langle K\rangle - \{\kappa_\sigma(\varepsilon_\sigma - \varepsilon_{\mathrm{Q}} + u_0 - \lambda_\sigma) \\ - \kappa_\sigma(\varepsilon_\sigma - \varepsilon_{\mathrm{Q}} - \lambda_\sigma)\}\langle n_\sigma\rangle\langle N_{\mathrm{Q}} - K\rangle, \end{aligned} \tag{39}$$

where $\kappa_\sigma(\varepsilon)$ is the Marcus rate for electron transfer between the site $\sigma$ and the interaction site Q,

$$\kappa_\sigma(\varepsilon) = |\Delta_\sigma|^2 \sqrt{\frac{\pi}{\lambda_\sigma T}}\, \exp\left(-\frac{\varepsilon^2}{4\lambda_\sigma T}\right). \tag{40}$$

The proton term $\Phi_\alpha$ is determined by the expression, similar to equation (39), as

$$\begin{aligned} \Phi_\alpha = \kappa_\alpha(E_\alpha - E_{\mathrm{Q}} + \Lambda_\alpha)\langle N_{\mathrm{Q}}\rangle\langle 1 - N_\alpha\rangle \\ - \kappa_\alpha(E_\alpha - E_{\mathrm{Q}} - \Lambda_\alpha)\langle 1 - N_{\mathrm{Q}}\rangle\langle N_\alpha\rangle \\ + \{\kappa_\alpha(E_\alpha - E_{\mathrm{Q}} + u_0 + \Lambda_\alpha) \\ - \kappa_\alpha(E_\alpha - E_{\mathrm{Q}} + \Lambda_\alpha)\}\langle 1 - N_\alpha\rangle\langle K\rangle \\ - \{\kappa_\alpha(E_\alpha - E_{\mathrm{Q}} + u_0 - \Lambda_\alpha) \\ - \kappa_\alpha(E_\alpha - E_{\mathrm{Q}} - \Lambda_\alpha)\}\langle N_\alpha\rangle\langle n_{\mathrm{Q}} - K\rangle, \end{aligned} \tag{41}$$

where $\kappa_\alpha(E)$ is the proton Marcus rate for the transitions between the site $\alpha$ and the proton-binding site Q,

$$\kappa_\alpha(E) = |\Delta_\alpha|^2 \sqrt{\frac{\pi}{\Lambda_\alpha T}}\, \exp\left(-\frac{E^2}{4\Lambda_\alpha T}\right). \tag{42}$$

*2.2.4. Equation for the electron–proton correlation function.* For the correlator, $\langle K\rangle$, of the electron ($n_{\mathrm{Q}}$) and proton ($N_{\mathrm{Q}}$) populations of the interaction site, we derive the following equation:

$$\langle \dot{K}\rangle = \mathcal{F}_{\mathrm{L}} + \mathcal{F}_{\mathrm{R}} + \mathcal{F}_{\mathrm{A}} + \mathcal{F}_{\mathrm{B}}, \tag{43}$$

where

$$\begin{aligned} \mathcal{F}_\sigma = \kappa_\sigma(\varepsilon_\sigma - \varepsilon_{\mathrm{Q}} + u_0 - \lambda_\sigma)\langle n_\sigma\rangle\langle N_{\mathrm{Q}} - K\rangle \\ - \kappa_\sigma(\varepsilon_\sigma - \varepsilon_{\mathrm{Q}} + u_0 + \lambda_\sigma)\langle 1 - n_\sigma\rangle\langle K\rangle, \\ \mathcal{F}_\alpha = \kappa_\alpha(E_\alpha - E_{\mathrm{Q}} + u_0 - \Lambda_\alpha)\langle N_\alpha\rangle\langle n_{\mathrm{Q}} - K\rangle \\ - \kappa_\alpha(E_\alpha - E_{\mathrm{Q}} + u_0 + \Lambda_\alpha)\langle 1 - N_\alpha\rangle\langle K\rangle. \end{aligned} \tag{44}$$

*2.2.5. Electron and proton currents.* Electron currents $I_{\mathrm{S}}$, $I_{\mathrm{D}}$ and proton currents $I_{\mathrm{N}}$, $I_{\mathrm{P}}$ are determined by an increase of the number of particles, electrons or protons, in the corresponding reservoir. In particular, a variation of the electron number in the drain lead gives a current

$$I_{\mathrm{D}} = \frac{\mathrm{d}}{\mathrm{d}t} \sum_k \langle c_{k\mathrm{D}}^{\dagger} c_{k\mathrm{D}}\rangle = \gamma_{\mathrm{D}}[\langle n_{\mathrm{R}}\rangle - f_{\mathrm{D}}(\varepsilon_{\mathrm{R}})], \tag{45}$$

whereas the proton current $I_{\mathrm{P}}$ is given by

$$I_{\mathrm{P}} = \frac{\mathrm{d}}{\mathrm{d}t} \sum_q \langle d_{q\mathrm{P}}^{\dagger} d_{q\mathrm{P}}\rangle = \Gamma_{\mathrm{P}}[\langle N_{\mathrm{B}}\rangle - F_{\mathrm{P}}(E_{\mathrm{B}})]. \tag{46}$$

Here,

$$\gamma_{\mathrm{D}} = 2\pi \sum_k |t_{k\mathrm{D}}|^2 \delta(\varepsilon_{\mathrm{R}} - \varepsilon_{k\mathrm{D}}),$$

and

$$\Gamma_{\rm P} = 2\pi \sum_q |T_{q\rm P}|^2 \delta(E_{\rm B} - E_{q\rm P})$$

are the electron ($\gamma_{\rm D}$) and proton ($\Gamma_{\rm P}$) transfer rates between the electron site R and the lead D, and between the proton-binding site B and the P-side of the membrane, respectively. The multiplications of the particle currents introduced above by the electron or proton charges produce the standard electric currents.

It follows from equations (36) and (37) that, in the steady-state, we have the relations

$$\langle \dot{n}_\sigma \rangle = 0, \qquad \langle \dot{N}_\alpha \rangle = 0,$$

so that

$$\Phi_{\rm L} + \Phi_{\rm R} = 0, \qquad \Phi_{\rm A} + \Phi_{\rm B} = 0,$$

and

$$I_{\rm S} = (\mathrm{d}/\mathrm{d}t) \sum_k \langle c^\dagger_{k\rm S} c_{k\rm S} \rangle = -I_{\rm D},$$
$$I_{\rm N} = (\mathrm{d}/\mathrm{d}t) \sum_q \langle d^\dagger_{q\rm N} d_{q\rm N} \rangle = -I_{\rm P}.$$

*2.2.6. Quantum yield of the electron-driven proton pump.* The productivity of the proton pump is determined by a quantum yield,

$$\mathrm{QY} = \frac{I_{\rm P}}{I_{\rm D}}, \tag{47}$$

and by the power-conversion efficiency $\eta$,

$$\eta = \mathrm{QY} \times \frac{\mu_{\rm P} - \mu_{\rm N}}{\mu_{\rm S} - \mu_{\rm D}}. \tag{48}$$

With standard conditions, we have

$$\mu_{\rm P} - \mu_{\rm N} = V_{\rm p} + 60\ \mathrm{meV} = 210\ \mathrm{meV},$$

and

$$\mu_{\rm S} - \mu_{\rm D} = V_{\rm e} = 600\ \mathrm{meV},$$

therefore,

$$\eta \simeq 0.35 \times \mathrm{QY}.$$

If a quantum yield (QY) is of order 1 (or 100%), the power-conversion efficiency $\eta$ may be as much as 0.35 (or 35%).

*2.3. Langevin equation*

For the redox-loop mechanism of a proton translocation through the membrane, the electron and proton sites, labeled by the letter Q, are attached to the shuttle: a molecule diffusing between the N and P sides of the membrane (see figure 2). This Brownian motion can be described by the one-dimensional overdamped Langevin equation for the coordinate $x$ of the shuttle,

$$\zeta \dot{x} = -\frac{\mathrm{d}U_{\rm c}(x)}{\mathrm{d}x} - \langle (n_{\rm Q} - N_{\rm Q})^2 \rangle \frac{\mathrm{d}U_{\rm s}(x)}{\mathrm{d}x} + \xi. \tag{49}$$

We assume that the shuttle molecule moves along a line connecting the sites L and A, located at $x = -x_0$, and the sites R and B, both having the coordinate $x = x_0$. The borders of the membrane, at $x = \pm x_0$, are schematically shown in figure 2. In equation (49), $\zeta$ is the drag coefficient of the shuttle, and $\xi$ is the Gaussian fluctuation force, which is characterized by the zero-mean value, $\langle \xi \rangle = 0$, and the correlation function,

$$\langle \xi(t)\xi(t') \rangle = 2\zeta T \delta(t - t'),$$

proportional to the temperature $T$ of the environment. The diffusion coefficient $D$ of the shuttle is also proportional to the temperature: $D = T/\zeta$. The motion of the shuttle is restricted by the membrane walls, which are simulated by the confinement potential $U_{\rm c}(x)$,

$$U_{\rm c}(x) = U_{\rm c0}\left\{1 - \left[\exp\left(\frac{x - x_{\rm c}}{l_{\rm c}}\right) + 1\right]^{-1} + \left[\exp\left(\frac{x + x_{\rm c}}{l_{\rm c}}\right) + 1\right]^{-1}\right\}, \tag{50}$$

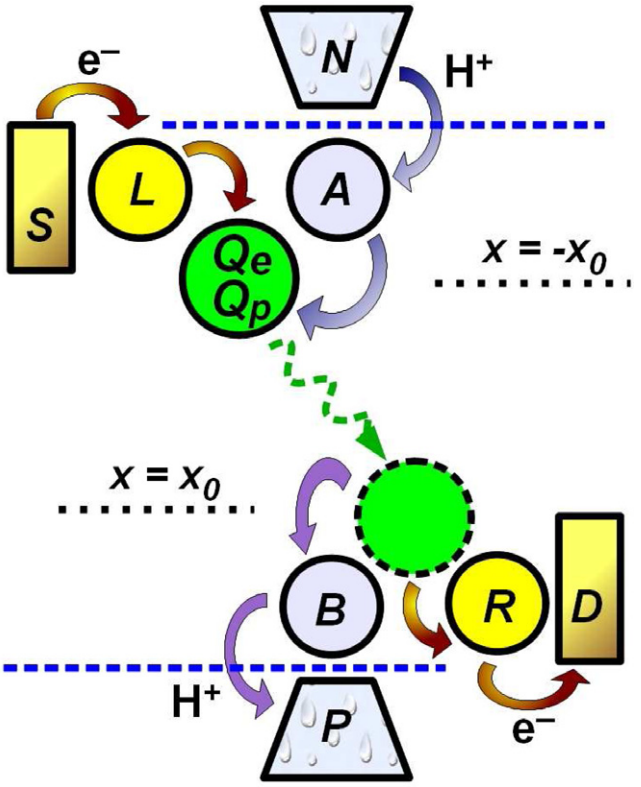


**Figure 2.** Schematic diagram of the redox-loop mechanism. Here, the electron–proton interaction site, Q = {$Q_e$, $Q_p$}, is placed on the molecular shuttle (shown in green), which diffuses along the line connecting the N and P sides of the membrane. From the source reservoir S, an electron $e^-$ jumps to the site L and, thereafter, to the shuttle, located at $x = -x_0$. The shuttle also accepts a proton $H^+$ transferred from the N-side of the membrane via the site A. The loaded shuttle moves randomly toward the P-side of the membrane, where (at $x = x_0$) the electron is subsequently transferred from the site $Q_e$ to the site R and to the drain reservoir D, and the proton jumps from the site $Q_p$ to the site B and, finally, to the P-side of the membrane. We note that, in this design, the electron site L and the proton site A are located near the N-side of the membrane (shown by the horizontal blue dashed line), and the electron site R and the proton site B are placed near the P-side.

having the barrier height $U_{c0}$, the width $2x_c$ ($x_c \geqslant x_0$) and the steepness $l_c$.

The potential barrier $U_s(x)$,

$$U_s(x) = U_{s0}\left\{\left[\exp\left(\frac{x - x_s}{l_s}\right) + 1\right]^{-1} - \left[\exp\left(\frac{x + x_s}{l_s}\right) + 1\right]^{-1}\right\}, \quad (51)$$

does not allow the shuttle with a non-zero charge $q = N_Q - n_Q$ (in units of $|e|$) to cross the lipid interior of the membrane. This barrier is determined by the height $U_{s0}$, the steepness $l_s$, and the width $2x_s$.

## 3. Results

We solve the rate equations (36) and (37) for the electron ($n_\sigma$) and proton ($N_\alpha$) populations jointly with the equation (43) for the electron–proton correlation function on the site Q, $K = \langle n_Q N_Q \rangle$. Our approach can describe two mechanisms of the redox-linked proton translocation across the membrane: (i) the static interaction site Q and (ii) the situation when the site Q diffuses between the sides of the membrane. The mechanism (i) roughly corresponds to the proton pump operating in *cytochrome c oxidase* (CcO) [3–6], whereas the design (ii) can be attributed to the redox-loop mechanism, which is responsible for electron and proton transfers in the inner membrane of bacteria [7–12].

### 3.1. Static proton pump

Here, we consider the mechanism (i), where the interaction site Q does not change its position (see figure 1). We assume that protons are transferred across the membrane, from the negatively charged side N, with an electrochemical potential $\mu_N$, to the positively charged side P, having an electrochemical potential $\mu_P$. All potentials and energies are measured in meV.

*3.1.1. Parameters.* The difference of electrochemical potentials, $\Delta\mu_H = \mu_P - \mu_N$, is determined by the following expression:

$$\Delta\mu_H = V_p - 2.3\,(RT/F) \times \Delta pH, \quad (52)$$

where $V_p$ is the transmembrane voltage, $R$ and $F$ are the gas and Faraday constants, respectively, $T$ is the temperature (in Kelvins, $k_B = 1$), and the concentration gradient $\Delta pH$ is about $-1$ [1, 2]. The coefficient $2.3\,(RT/F)$ is about 60 meV at room temperature, $T = T_0 \equiv 298$ K. It follows from equation (52) that the potentials of the N and P sides of the membrane can be written as

$$\mu_N = -\mu_{H0} - \Delta V_p/2 - 30 \times (\Delta T/T_0),$$
$$\mu_P = \mu_{H0} + \Delta V_p/2 + 30 \times (\Delta T/T_0), \quad (53)$$

where $\Delta V_p = V_p - V_0$, $\Delta T = T - T_0$. At the standard conditions, when $T = T_0$, $V_p = V_0 = 150$ meV, for the electrochemical potential $\mu_{H0}$ we have: $\mu_{H0} = 105$ meV. Thus, the total proton gradient across the membrane, $\Delta\mu_H$, is about 210 meV. As in the CcO proton pump [3, 6], we assume that the proton-binding sites A, $Q_p$, and B are located approximately on the line connecting the N and P sides of the membrane with the following coordinates: $x_A = 0.1$, $x_Q = 0.3$, $x_B = 0.5$. The coordinates of the sites are counted from the middle of the membrane in a direction towards the P-side and are measured in units of the membrane width $W$ with $W \simeq 4$ nm. Protons are delivered from the N-side to the site A by the so-called D-pathway crossing about a half of the membrane. We also note that the B-site is located next to the P-side (see figure 1). An influence of the transmembrane voltage $V_p$ on the energy levels of the proton sites is described by the formulas

$$E_A = E_{A0} + x_A \times \Delta V, \qquad E_Q = E_{Q0} + x_Q \times \Delta V,$$
$$E_B = E_{B0} + x_B \times \Delta V. \quad (54)$$

For the proton energy levels, $E_{A0}$, $E_{Q0}$, and $E_{B0}$, at the voltage $V_p = V_0$, we assume the following values (in meV): $E_{A0} = -155$, $E_{Q0} = 250$, and $E_{B0} = 185$, unless otherwise specified. This means that at the standard conditions, the proton begins its journey at the N-side with the potential $\mu_N = -105$ meV and jumps to the A-site having a lower energy ($-155$ meV). However, the next proton-binding site $Q_p$ has a much higher energy ($\sim$250 meV), so that the proton transfer cannot occur without a mediation of the electron component. The electron site $Q_e$ is electrostatically coupled to the proton-binding site $Q_p$ with the Coulomb energy $u_0$. Thus, in the presence of an electron on the site $Q_e$ the energy of the Q-proton decreases to the level $E_{Q0} - u_0 \simeq -220$ meV, provided that $u_0 \simeq 470$ meV. Now the proton can move from site A to site Q, since $E_{A0} > E_{Q0} - u_0$. Depopulation of the electron site Q returns the energy level of the Q-proton to its original value $E_{Q0} = 250$ meV, which is higher than the energy level of the next-in-line B-site, $E_{B0} = 185$ meV, and is *much higher* than the energy level of the A-site. We assume that the backward proton transfer (from $Q_p$ to the A-site) is described by the *inverted region* of the Marcus formula, so that the probability of such transfer is low compared to the probability of the proton transfer from the site $Q_p$ to the site B. No additional gate mechanism is necessary here.

For the sake of simplicity, we assume that three electron-binding sites L, $Q_e$, R as well as the source and drain leads are positioned on a line, which is parallel to the surface of the membrane (see figure 1). Thus, the transmembrane gradient $V_p$ has no effect on electron transport from the electron source S to the drain D. For the potentials of the electron reservoirs, we choose the following form:

$$\mu_S = \mu_{e0} + V_e/2, \qquad \mu_D = \mu_{e0} - V_e/2, \quad (55)$$

with $\mu_{e0} = -500$ meV and with the electron voltage gradient $V_e = 600$ meV, unless otherwise indicated. The electron voltage gradient $V_e$ roughly corresponds to the drop of the redox potential along the electron transfer chain in the *cytochrome c oxidase* [1–3]. We assume that the electron pathway includes the source reservoir ($\mu_S = -200$ meV), the site L ($\varepsilon_L = -210$ meV), the interaction site $Q_e$ ($\varepsilon_Q = -250$ meV),

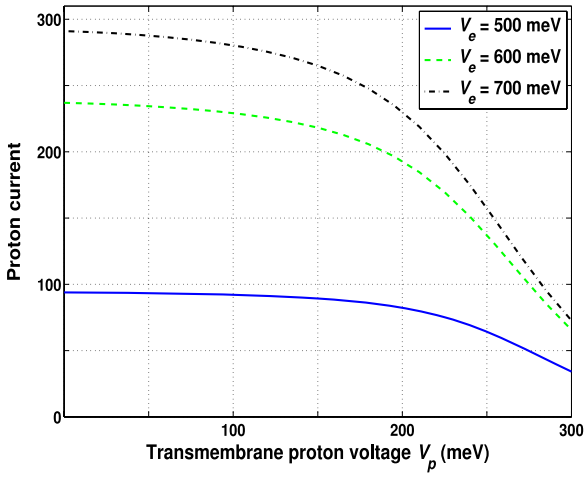


**Figure 3.** Proton current versus transmembrane voltage $V_\mathrm{p}$ at room temperature, $T = 298$ K, and three different electron potentials: $V_\mathrm{e} = 500$, 600, and 700 meV. The proton current is almost constant for low values of $V_\mathrm{p}$, and decreases for increasing $V_\mathrm{p}$.

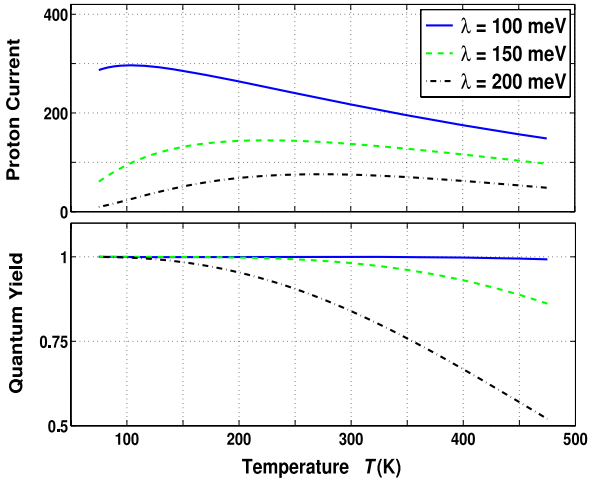


**Figure 4.** Proton current (the number of protons translocated across the membrane per 1 $\mu$s) and QY versus temperature for the electron voltage $V_\mathrm{e} = 600$ meV, transmembrane proton voltage $V_\mathrm{p} = 150$ meV, and three different reorganization energies: $\lambda = 100$, 150, and 200 meV. The proton current and QY both decrease for increasing $\lambda$.

the site R ($\varepsilon_\mathrm{R} = -770$ meV), and the electron drain reservoir having the potential $\mu_\mathrm{D} = -800$ meV.

We assume that the electron and proton transfer between the active sites, L–Q, R–Q and A–Q, B–Q, are quite fast, with amplitudes $\Delta_\mathrm{L} \simeq \Delta_\mathrm{R} \simeq 0.3$ ps$^{-1}$ and $\Delta_\mathrm{A} \simeq \Delta_\mathrm{B} \simeq 0.3$ ps$^{-1}$, whereas the transitions to and out of the electron and proton reservoirs are characterized by much slower rates: $\gamma_\mathrm{S} \simeq \gamma_\mathrm{D} \simeq 1.5$ ns$^{-1}$, and $\Gamma_\mathrm{N} \simeq \Gamma_\mathrm{D} \simeq 0.75$ ns$^{-1}$. The responses of the environment to the electron and proton transitions are described by the corresponding reorganization energies: $\lambda_\mathrm{L} = \lambda_\mathrm{R} = \lambda_\mathrm{e}$ and $\Lambda_\mathrm{A} = \Lambda_\mathrm{B} = \Lambda_\mathrm{p}$, respectively. Here, for the standard case, we assume that $\lambda_\mathrm{e} \simeq 100$ meV and $\Lambda_\mathrm{p} \simeq 100$ meV. This set of parameters provides an efficient operation of the redox-linked proton pump.

*3.1.2. Dependence of the proton current on the transmembrane voltage.* In figure 3, we show the steady-state proton current $I_\mathrm{P}$ as a function of the transmembrane voltage gradient $V_\mathrm{p}$, at three different values of the electron voltage: $V_\mathrm{e} = 500$, 600, 700 meV. We use here the standard set of other parameters (see section 3.1.1), where $T = 298$ K and $\lambda_\mathrm{e} = \Lambda_\mathrm{p} = 100$ meV.

The proton current $I_\mathrm{P}$ is equal to the number of protons pumped *energetically uphill* (at $V_\mathrm{p} > 0$), from the N-side to the P-side of the membrane, *per one microsecond*. At the difference $V_\mathrm{e} = 600$ meV of source and drain redox potentials, the system pumps more than 200 protons per 1 $\mu$s against the transmembrane voltage gradient $V_\mathrm{p} = 150$ meV. According to equation (53), this voltage corresponds to the proton electrochemical gradient $\Delta\mu_H = 210$ meV, which is usually applied to the internal membrane of mitochondria and the plasma membranes of bacteria. The number of pumped protons goes down as the proton voltage $V_\mathrm{p}$ increases, and goes up with increasing electron voltage difference $V_\mathrm{e}$. The proton current saturates at $V_\mathrm{e} > 750$ meV. It is evident from figure 3 that at high enough electron voltages ($V_\mathrm{e} \geqslant 600$ meV), the pump is able to translocate more than 100 protons per microsecond against the proton gradient $V_\mathrm{p}$, exceeding 250 meV ($\Delta\mu > 310$ meV). The QY is about 1 (with a power-conversion efficiency $\eta \simeq 35\%$) in the whole region of electron and proton voltages: 500 meV $< V_\mathrm{e} <$ 800 meV, 0 meV $< V_\mathrm{p} <$ 300 meV.

*3.1.3. Proton current and quantum yield as functions of temperature.* Figure 4 shows the pumping proton current, $I_\mathrm{P}$ (i.e., the number of protons translocated from the N- to the P-side of the membrane per 1 $\mu$s) versus the temperature $T$ measured in Kelvins. The graphs are presented at three values of the electron and proton reorganization energy: $\lambda = 100$, 150, 200 meV. We assume here that $\lambda_\mathrm{e} = \Lambda_\mathrm{p} = \lambda$, with the electron voltage $V_\mathrm{e} = 600$ meV and the proton gradient $V_\mathrm{p} = 150$ meV. It is of interest that at $\lambda \geqslant 150$ meV the pumping current has a pronounced maximum near room temperature, 200 K $< T <$ 300 K, although the QY is higher, QY $\sim 1$, at lower temperatures. The performance of the pump deteriorates at higher reorganization energies when the coupling to the environment increases. Increasing the reorganization energy leads to an increased probability for an electron to be transferred through the system, losing all its excess energy to the environment without transferring this energy to protons. Such a probability is further increased at large temperatures leading to the observed decrease of the QY.

*3.1.4. Dependence of the proton current on the parameters of the interaction site.* The energy transfer from the electron to the proton component occurs on the interaction site $\mathrm{Q} = \{\mathrm{Q_e}, \mathrm{Q_p}\}$, which has one electron ($\varepsilon_\mathrm{Q}$) and one proton ($E_\mathrm{Q}$) energy level (see equation (54)). The electron on the site $\mathrm{Q_e}$ is electrostatically coupled to the proton, which populates the site $\mathrm{Q_p}$, with the Coulomb energy $u_0$. It follows from figure 5 that the proton pumping current $I_\mathrm{P}$ exhibits a resonant behavior as a function of the charging energy $u_0$ and the position of the proton energy level $E_{\mathrm{Q}0}$. The dependence of the pumping

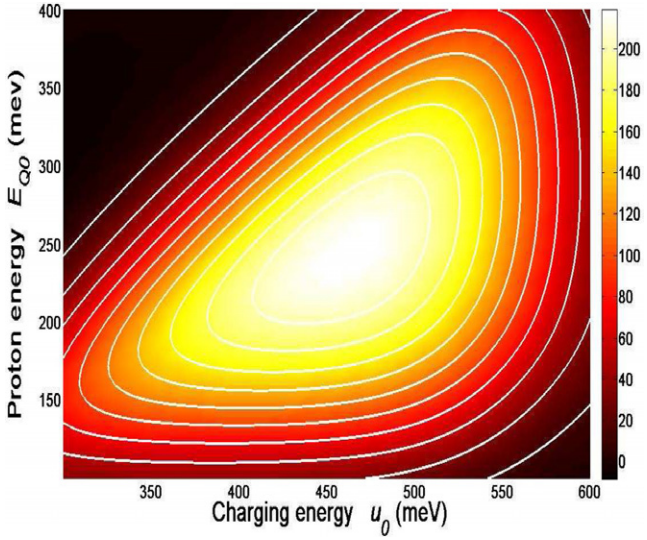


**Figure 5.** Dependence of the proton current (the number of protons pumped across the membrane per one $\mu$s, see the color bar on the right side) on the charging energy $u_0$, and on the energy $E_{Q0}$ of the central proton site for $V_e = 600$ meV, $V_p = 150$ meV, and $T = 298$ K.

current on the electron energy $\varepsilon_Q$ has a resonant character as well. Here we assume that $V_e = 600$ meV, $V_p = 150$ meV, $\lambda_e = \Lambda_p = 100$ meV, and $T = 298$ K. The energetically uphill proton current has a pronounced maximum ($I_P \simeq 220\ \mu s^{-1}$) at the Coulomb energy $u_0 = 470$ meV and the proton energy $E_{Q0} = 250$ meV, provided that the electron energy $\varepsilon_Q = -250$ meV. It is important that the proton pump is robust to the variations of the Coulomb energy $u_0$ and the proton energy $E_{Q0}$ in the range $\pm 50$ meV from the resonant values. The QY is very close to one in the central region of figure 5, so that the power-conversion efficiency $\eta$ is about 35%.

Figures 3–5 clearly demonstrate that, at standard physiological conditions, the static redox-linked proton pump ('CcO-pump') efficiently converts the energy of electrons to the more stable energetic form of the proton electrochemical gradient across the membrane.

### *3.2. Redox-loop mechanism of electron and proton translocation*

In many biological systems, electrons and protons can be transferred across a membrane by means of a molecular shuttle diffusing inside the membrane, from one side to another. Here we show that the mathematical model described in section 2 can be successfully applied for a description of the redox-loop mechanism, which utilizes the Brownian motion of the shuttle Q carrying both electron, $Q_e$, and proton, $Q_p$, sites (see figure 2). As in the previous case, we have to solve here a system of master equations for the electron ($n_L$, $n_Q$, $n_R$) and proton ($N_A$, $N_Q$, $N_B$) populations, equations (36) and (37), and for the correlation function $K$ of electron and proton populations on the site Q, equation (43). However, these master equations should be complemented by the Langevin equation, equation (49), for the time-dependent shuttle position $x$. We note that the electron tunneling between the sites L–Q, Q–R, as well as the proton transfer rates between the sites A–Q and Q–B, depend on the position $x$ of the shuttle.

*3.2.1. Parameters.* We assume that the electron site L is located near the N-side of the membrane, at $x = -x_0$, where $x_0 = 2$ nm. The other electron site R is near the P-side of the membrane, at $x = +x_0$. The reservoir S, connected to the site L, serves as a source of electrons, and the reservoir D, coupled to the site R, serves as an electron drain (see figure 2). The tunneling amplitudes $\Delta_L$, $\Delta_R$ are determined by the amplitudes $\Delta_{L0}$, $\Delta_{R0}$, and by the electron tunneling length $l_e$:

$$\Delta_L(x) = \Delta_{L0} \times \exp\left(-\frac{|x + x_0|}{l_e}\right),$$
$$\Delta_R(x) = \Delta_{R0} \times \exp\left(-\frac{|x - x_0|}{l_e}\right). \tag{56}$$

The proton-binding site A is located at the end of the N-side proton pathway, whereas the site B terminates a pathway, which goes into the P-side of the membrane. For the $x$-dependences of the proton transfer amplitudes $\Delta_A$ and $\Delta_B$, we choose the following relations:

$$\Delta_A(x) = \Delta_{A0} \times \left[\exp\left(\frac{x_0 + x}{l_p}\right) + 1\right]^{-2},$$
$$\Delta_B(x) = \Delta_{B0} \times \left[\exp\left(\frac{x_0 - x}{l_p}\right) + 1\right]^{-2}, \tag{57}$$

where $l_p$ is the proton transfer length. It should be noted that our model produces the same results when the proton amplitudes are given by expressions similar to equations (56). For the transfer parameters, we choose the following values: $\Delta_{L0} \sim \Delta_{R0} = 0.04$ meV, $\Delta_{A0} \sim \Delta_{B0} = 0.04$ meV, and $l_e = 0.25$ nm, $l_p = 0.25$ nm. Couplings to the electron and proton reservoirs are described by the rates $\gamma_S \sim \gamma_D = 0.5\ ns^{-1}$ and $\Gamma_N \sim \Gamma_P = 0.1\ ns^{-1}$. The system is robust to significant variations of the transfer parameters.

The confinement potential $U_c(x)$ is determined by the height $U_c = 500$ meV, the steepness $l_c = 0.1$ nm, and the half-width $x_c = 2.7$ nm. The potential barrier $U_s(x)$, preventing the charged shuttle from entering into the membrane, is characterized by the height $U_s = 770$ meV, the width $x_s = 1.7$ nm, and the steepness $l_s = 0.05$ nm.

Accordingly, the electron and proton populations of the shuttle are almost completely compensated, $n_Q \simeq N_Q$, so that the potential $U_s(x)$ gives a negligible contribution to the energies of electrons and protons. However, we have to take into account the fact that in the presence of the voltage gradient, $V_p \simeq 150$ meV, the electron ($\varepsilon_Q$) and proton ($E_Q$) energies on the moving shuttle depend on the shuttle position $x$:

$$\varepsilon_Q = \varepsilon_{Q0} - \frac{x}{2x_0}V_p, \qquad E_Q = E_{Q0} + \frac{x}{2x_0}V_p, \tag{58}$$

with $\varepsilon_{Q0} = 280$ meV, and $E_{Q0} = u_0/2 = 200$ meV, where for the charging energy $u_0$ of the shuttle we have: $u_0 = 400$ meV.

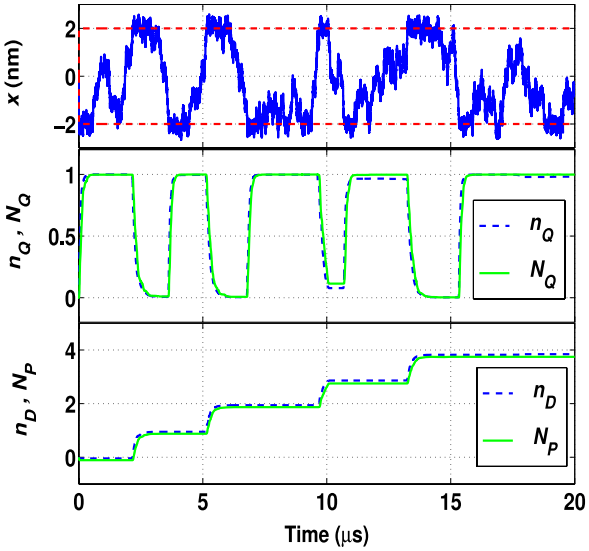


**Figure 6.** Time evolution of the electron–proton translocation process. Here $x$ is the location of the shuttle, $n_Q$ and $N_Q$ are the electron and proton populations of the shuttle, respectively, $n_D$ is the number of electrons transferred from the electron source S to the electron drain D, and $N_P$ is the number of protons translocated from the N- to the P-side of the membrane. It can be seen from this figure that the loading/unloading of the shuttle with electrons and protons, as well as the electron and proton transfer across the membrane, are clearly correlated with the spatial motion of the shuttle.

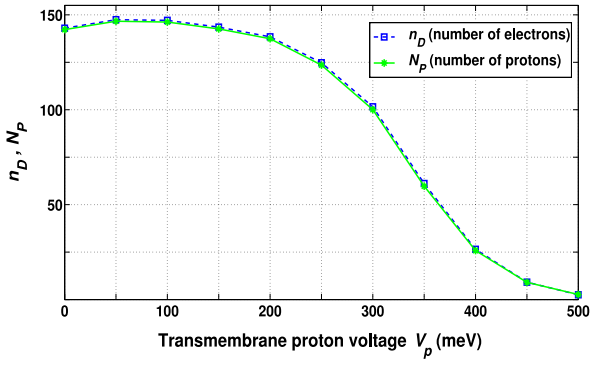


**Figure 7.** Numbers of electrons, $n_D$, and protons, $N_P$, translocated across the membrane in one millisecond, versus the transmembrane proton voltage $V_p$ at room temperature, $T = 298$ K, and at $(\mu_S - \mu_D) = 650$ meV. Clearly, it is much harder to transfer protons against the higher transmembrane voltages.

Thus, electrons move from the source reservoir, having the electrochemical potential $\mu_S = 420$ meV, to the L-site (with the energy $\varepsilon_L = 380$ meV), and, thereafter, to the shuttle. On the opposite side of the membrane, the electron, populating the shuttle, jumps to the site R ($\varepsilon_R = -170$ meV) and, finally, to the drain reservoir ($\mu_D = -230$ eV). The total drop of the redox potential in this electron-transport chain can be estimated as $\mu_S - \mu_D = 650$ meV.

Protons move from the N-side of the membrane ($\mu_N = -105$ meV) to the site A, having a lower energy $E_A = -150$ meV. The energy level $E_Q = 125$ meV of the proton on the shuttle, located near the N-side of the membrane (at $x = -x_0$), is much higher than $E_A$, if the shuttle contains no electrons. However, the shuttle populated with a single electron is more attractive for protons, since in this case the effective energy of the proton, $E_Q - u_0 = -275$ meV, is less than the energy of the proton-binding site A. The shuttle, carrying one electron and one proton, diffuses to the opposite side of the membrane ($x = +x_0$), where the electron, with energy $\varepsilon_Q - u_0 = -195$ meV, is able to tunnel to the site R, having a slightly higher energy $\varepsilon_R = -170$ meV. In the absence of an electron, the energy of the proton on the shuttle (at $x = +x_0$) increases to the level $E_Q = E_{Q0} + V_p/2 = 275$ meV, which exceeds the energy of the proton on the site B: $E_B = 150$ meV. Consequently, the proton moves from the shuttle to the site B and, thereafter, to the P-side of the membrane characterized by the electrochemical potential $\mu_P = +105$ meV. Thus, this redox-loop mechanism translocates protons across the membrane against the proton electrochemical gradient $\Delta\mu_H = \mu_P - \mu_N = 210$ meV, and against the transmembrane potential $V_p \sim 150$ meV.

*3.2.2. Proton translocation process.* Figure 6 exhibits the electron and proton populations of the shuttle, $n_Q(t)$ and $N_Q(t)$, correlated with the shuttle's position $x(t)$ at $T = 298$ K, $V_p = 150$ meV, and at $\Delta\mu = 210$ meV. In this figure, we also show the time dependences of the number of electrons, $n_D(t)$, transferred to the drain reservoir, and the number of protons, $N_P(t)$, translocated to the P-side of the membrane. The shuttle diffuses between the membrane walls located at $x = \pm x_0$ ($x_0 = 2$ nm) with an average crossing time $\Delta t \sim 2.5$ $\mu$s. This timescale is closely related to the diffusion time,

$$t_D \sim \langle \Delta x^2 \rangle / 2D \sim 2.66\ \mu\text{s},$$

obtained at $\sqrt{\langle \Delta x^2 \rangle} \sim 2x_0 = 4$ nm, for the diffusion coefficient of the quinone molecule $D \sim 3 \times 10^{-12}$ m$^2$ s$^{-1}$.

At $t \sim 0$, the shuttle, located at $x \sim -x_0$, is loaded with one electron and one proton taken from the N-side of the membrane (see figure 2). When $t \sim 2.5$ $\mu$s, the shuttle reaches the P-side ($x = +x_0 = 2$ nm) and unloads the electron to the site R (and later to the drain lead D) and the proton to the site B, coupled to the P-side of the membrane. Consequently, the population $N_P$ of the P-side grows. The empty shuttle diffuses back to the N-side, completing the cycle, and the process starts again. In 20 $\mu$s, the shuttle performs four complete trips and translocates about four electrons and four protons across the membrane.

*3.2.3. Voltage and temperature dependences.* The numbers of electrons and protons, $n_D$ and $N_P$, respectively, transferred across the membrane in one millisecond, are shown in figure 7 as functions of the transmembrane proton voltage $V_p$. The electrochemical gradient of protons, $\Delta\mu = \mu_P - \mu_N$, is proportional to $V_p$: $\Delta\mu \simeq V_p + 60$ meV (at $T = 298$ K). The results in figure 7 are averaged over ten realizations. The system is able to translocate more than 120 protons ms$^{-1}$ against the high transmembrane voltage, $V_p \leqslant 250$ meV, that corresponds to the electrochemical gradient $\Delta\mu \leqslant 310$ meV.

It follows from figure 8 that the translocation mechanism works efficiently in a wide range of temperatures, 250 K $< T <$ 500 K. In this range, the system pumps more than

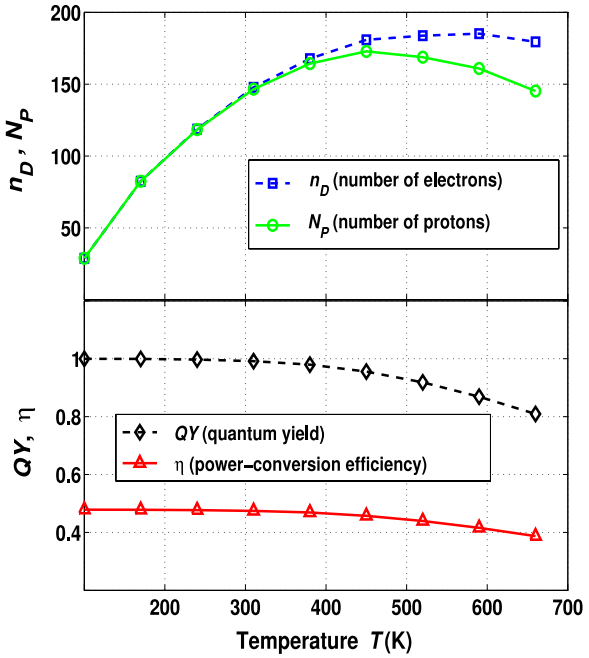


**Figure 8.** Temperature dependence of the numbers of electrons, $n_D$, and protons, $N_P$, transferred across the membrane by the diffusing shuttle, at $V_p = 150$ meV and $(\mu_S - \mu_D) = 650$ meV. We also present here the QY and the power-conversion efficiency, $\eta$, of the process as functions of the temperature. At higher temperatures, the shuttle moves faster and carries more electrons and more protons. However, if the temperature is too high, the shuttle does not have enough time to be loaded with electrons and protons, and sometimes travels empty. As a result of this, the electron and proton currents decrease at high temperatures, thus decreasing the efficiency of the pump.

120 protons ms$^{-1}$ with a QY exceeding 90% and with a power-conversion efficiency $\eta$ higher than 40%. With increasing temperature, the shuttle performs more trips between the sides of the membrane, thus carrying more electrons and protons. This increases the proton current (i.e., the number of protons translocated per unit time). We note that the proton population of the shuttle exists only after loading the shuttle with an electron. At very high temperatures, $T > 500$ K, the shuttle moves quite fast, and protons have fewer chances to jump onto the shuttle. Consequently, the gap between electron and proton currents grows with the temperature, thus deteriorating the performance of the pump.

## 4. Conclusion

Two different mechanisms of energetically uphill proton translocation across a biomembrane are described by the same physical model. This model includes three redox sites (L, $Q_e$, R) and three proton-binding sites (A, $Q_p$, B) attached to the S and D electron reservoirs, as well as to the proton reservoirs on the P and N sides of the membrane. We have shown that it is the strong Coulomb interaction between the electron site $Q_e$ and the proton site $Q_p$ which plays the most prominent role in the process of energy transformation from electrons to protons. In this case, the whole electron–proton transport chain can be divided into weakly coupled clusters of sites, so that the total number of occupation states is equal to the sum (not to the product) of occupation states in each cluster. With physiological conditions, our model demonstrates a proton pumping effect with a QY near 100% and a power-conversion efficiency of the order of 35%, for both the static proton pump, related to the *cytochrome c oxidase*, as well as for the redox-loop mechanism, where electrons and protons are translocated by the diffusing molecular shuttle.

## Acknowledgments

This work was supported in part by the Laboratory of Physical Sciences, National Security Agency, Army Research Office, National Science Foundation grant No. 0726909, JSPS-RFBR contract No. 09-02-92114, Grant-in-Aid for Scientific Research (S), MEXT Kakenhi on Quantum Cybernetics, and Funding Program for Innovative R&D on S&T (FIRST). LM was partially supported by the NSF NIRT, grant No. ECS-0609146 and by the PSC-CUNY award No. 41-613.

## References

[1] Alberts B, Johnson A, Lewis J, Raff M, Roberts K and Walter P 2002 *Molecular Biology of the Cell* (New York: Garland Science) chapter 14
[2] Nicholls D G and Ferguson S J 2002 *Bioenergetics* vol 3 (London: Academic)
[3] Wikström M and Verkhovsky M I 2007 *Biochim. Biophys. Acta* **1767** 1200
[4] Belevich I, Bloch D A, Belevich N, Wikström M and Verkhovsky M I 2007 *Proc. Natl Acad. Sci. USA* **104** 2685
[5] Kim Y C, Wikström M and Hummer G 2007 *Proc. Natl Acad. Sci. USA* **104** 2169
[6] Smirnov A Yu, Mourokh L G and Nori F 2009 *J. Chem. Phys.* **130** 235105
[7] Mitchell P 1976 *J. Theor. Biol.* **62** 327
[8] Jormakka M, Törnroth S, Byrne B and Iwata S 2002 *Science* **295** 1863
[9] Bertero M G, Rothery R A, Palak M, Hou C, Lim D, Blasco F, Weiner J H and Strynadka N C 2003 *Nature Struct. Molec. Biol.* **10** 681
[10] Gennis R B 2005 *Biophysical and Structural Aspects of Bioenergetics* ed M Wikström (Cambridge: RSC Publishing)
[11] Smirnov A Yu, Savel'ev S and Nori F 2009 *Phys. Rev.* E **80** 011916
[12] Ghosh P K, Smirnov A Yu and Nori F 2009 *J. Chem. Phys.* **131** 035102
[13] Smirnov A Yu, Mourokh L G and Nori F 2008 *Phys. Rev.* E **77** 011919
[14] Johansson J R, Mourokh L G, Smirnov A Yu and Nori F 2008 *Phys. Rev.* B **77** 035428
[15] Cherepanov D A, Krishtalik L I and Mulkidjanian A Y 2001 *Biophys. J.* **80** 1033